NANO LETTERS

Letter

pubs.acs.org/NanoLett

Molecular Scale Conductance Photoswitching in Engineered Bacteriorhodopsin

Olivia Berthoumieu,[†] Amol V. Patil,[‡] Wang Xi,[‡] Lubica Aslimovska,[†] Jason J. Davis,*[,‡] and Anthony Watts*[,†]

[†]Department of Biochemistry, University of Oxford, South Parks Road, Oxford OX1 3QU, United Kingdom

[‡]Department of Chemistry, Physical and Theoretical Chemistry Laboratory, University of Oxford, South Parks Road, Oxford OX1 3QZ, United Kingdom

Supporting Information

ABSTRACT: Bacteriorhodopsin (BR) is a robust light-driven proton pump embedded in the purple membrane of the extremophilic archae *Halobacterium salinarium*. Its photoactivity remains in the dry state, making BR of significant interest for nanotechnological use. Here, in a novel configuration, BR was depleted from most of its endogenous lipids and covalently and asymmetrically anchored onto a gold electrode through a strategically located and highly responsive cysteine mutation; BR has no indigenous cysteines. Chemisorption on gold was characterized by surface plasmon resonance, reductive striping voltammetry, ellipsometry, and atomic force microscopy (AFM). For the first time, the conductance of isolated protein trimers, intimately probed by conducting AFM, was reproducibly and reversibly switched under wavelength-specific conditions (mean resistance of 39 ± 12 MΩ under illumination, 137 ± 18 MΩ in the dark), demonstrating a surface stability that is relevant to potential nanodevice applications.

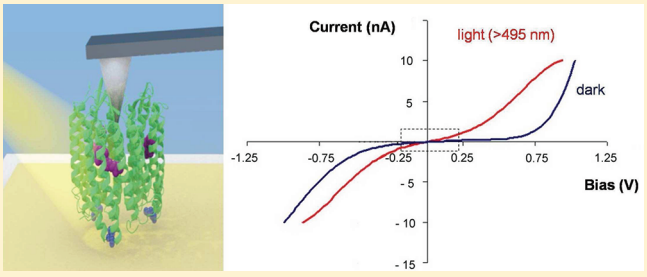

KEYWORDS: *Bacteriorhodopsin, conducting atomic force microscopy, molecular conductance photoswitching, wavelength sensitivity*

In biology, retinal/opsin and phytochrome systems display analogous photon-induced conformational changes.[1,2] The simplest and best described system is the retinal bound photoreceptor bacteriorhodopsin (BR), which acts as a light-driven proton pump in the extremophile archae, *Halobacterium salinarium*.[3] Retinal has a broad absorption band centered at 568 nm and is stoichiometrically linked via a Schiff base to each protein molecule.[4] Light absorption isomerizes the retinal chromophore from all-trans to 13-cis, initiating a cycle of conformational changes that lead to unidirectional proton pumping from the cytoplasmic to extracellular side of BR.[4−7] This mechanism produces an electrochemical gradient across the membrane that is used for ATP synthesis under anaerobic conditions. Although BR functions as a monomer,[7] these monomers are organized within the plasma membrane as a two-dimensional, hexagonal crystalline lattice of uniformly oriented trimers,[3−7] referred to as the purple membrane (PM). The proteins of extremophiles are inherently stable by virtue of their amino acid charge distribution and nonhydrolyzable protective ether linked lipids in membranes.[8,9] BR remains stable up to 80 °C in solution and 140 °C in dry state, across a 0−12 pH range and resists both high ionic strength and most forms of protease digestion.[7]

Photoinduced conformational changes through the BR photocycle have been extensively studied using a wide range of methods [X-ray diffraction, NMR, electron microscopy (EM), atomic force microscopy (AFM), electron spin resonance (ESR)].[6,10−13] The conformational changes in the receptor induce a charge separation that is coupled to proton transport[14] and involves a succession of charge displacements across the molecule resulting in a quantifiable photoelectric response.[7] Similarly, the photoresponse of a number of organic molecules, such as azobenzenes, spyropyrans and fulgides, triggers conformational changes that modulate the distance between electron donors and acceptors (for example, appended to the para position of phenylene rings in porphyrin−azobenzene−porphyrin[15] or azobenzene−porphyrin−azobenzene)[16] or between chromophore and electrodes in a proximal probe junction, to which, in most cases, current modulation of the reversible switching has been assigned.[17]

Scanning probe techniques present a powerful means of elucidating molecular scale properties. They have been reproducibly applied to the direct topographic imaging and conductance analyses of a range of surface-confined biomolecular systems[11,18,19] and played a significant role in the recent rise of nanotechnology. Previous conducting atomic force microscopy (C-AFM) analyses with metal-coated probes have specifically resolved and modeled protein conductance under a wide range of experimental conditions.[20−22] Attempts to engage monolayers of BR in the native PM for electronic measurements,

Received: November 10, 2011
Revised: December 7, 2011

 © XXXX American Chemical Society dx.doi.org/10.1021/nl203965w | *Nano Lett.* XXXX, XXX, XXX−XXX

through the use of either lithographically fabricated contacts or C-AFM probes, have led to reported junction resistances in the TΩ range[23] and low (pA range) currents per trimer.[20,23,24]

The photoactivity of BR is retained in dried films of PM,[25,26] making it an attractive material for developing biomolecular devices, such as photodetectors or optical memories.[7,27,28] In all previous work, to the best of our knowledge, the protein photoresponse has been analyzed in the PM, within relatively large (micrometer sized) patches or in PM dispersions contained in wells. We report here a controlled, orientated, and covalent surface immobilization of functionally competent, partially delipidated BR trimers that are bound to a gold surface and the analysis of their photoinduced conductance switching at molecular scales using C-AFM.

The lipid composition and density within the PM differ between the cytoplasmic and the extracellular side, both having different surface charges and stiffness as shown by AFM.[12] Homogeneous orientation, covalent and intimate chemisorption of BR_{cys} on a gold substrate, was achieved through a strategically engineered cysteine mutation at M163C (BR_{cys}); wild-type BR is devoid of any cysteine. The location of the mutation in the conformationally sensitive interhelix EF intracellular loop of BR[10] is expected to orient the transmembrane helices close to perpendicular to the conducting surface. High-speed AFM has confirmed this conformational sensitivity of the EF loop, indicating that real-time light-induced conformational changes occur in BR in PM, resulting in a counter-clockwise twist outward from the protein center upon illumination, with the loop being displaced by a greater distance (~0.8 nm) than the helices move.[11] Such distance and conformational sensitivity make this location of the immobilization site for switching electrical measurements more attractive than for more inert and less conformationally sensitive locations.

Partial detergent-mediated delipidation of BR is a nondestructive way of depleting the protein of 75% of its native highly charged lipids (mono- and disulfate and phosphate analogues, with residual negative charges 1 or 3),[8,9] while retaining endogenous lipids involved in the cohesion of the protein trimers. Partially delipidated BR is still thermally stable, as it is in PMs, with an unfolding temperature of ~94 °C;[8] the exposed, nonburied position of the cysteine mutation is not expected to change thermal stability significantly. An absorbance peak was observed at 560 nm for the partially delipidated sample in solution, as expected,[8] and a hypsochromic shift to 500 nm occurred after binding BR_{cys} onto gold (Supporting Information, Figure S1). This shift demonstrated that the cysteine mutant was bound to the gold substrate and retained its photon absorption characteristics. Surface plasmon resonance association curves (Supporting Information, Figure S2) showed that BR_{cys} and wild-type BR were both immobilized on a bare gold surface after injection. The amount of bound protein, after washing the gold chip with detergent buffer, was four times higher for BR_{cys} (protein density on the surface of 46.83 ± 3.33 ng/cm^2) than for wild-type BR (11.22 ± 1.52 ng/cm^2), an observation consistent with a robust thiolate-based immobilization with the former. Other studies, including AFM imaging (Figure 1), ellipsometry, and reductive stripping voltammetry (Supporting Information, Figure S3), were performed to assess the sample layer thickness and to provide further confirmation of the specific and orientated immobilization on gold of the BR_{cys} compared to wild-type BR. Additional Kelvin probe and photocurrent measurements

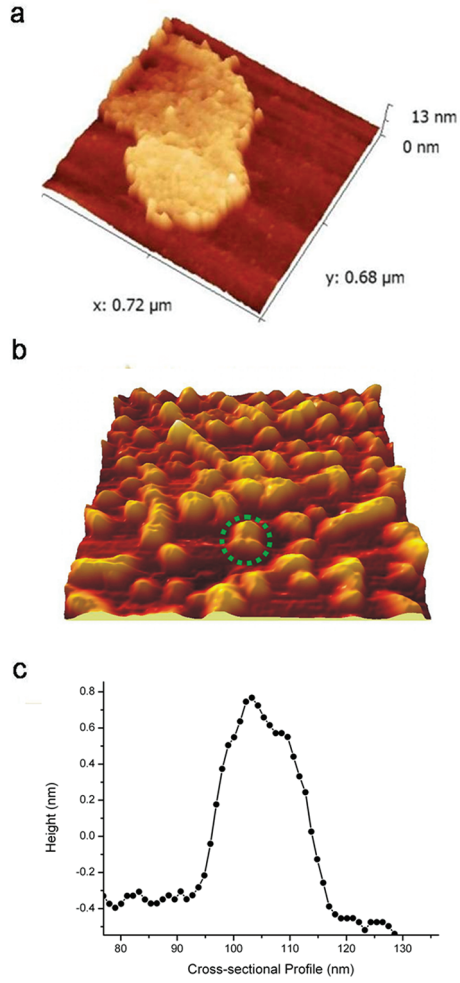

Figure 1. AFM imaging of BR on gold. Topographic image (tapping mode in air, Digital Instruments NanoScope IV microscope) of a (a) wild-type PM patch and (b) partially delipidated BR_{cys} on flame annealed gold on glass substrate (200 × 200 nm image). The BR_{cys} sample (10 μM) shows discrete BR trimers, or groups (up to 7) of trimers, with an average area of ~250 sq nm. (c) Topographical cross-section of the indicated trimer (green circle in b, xy scale 300 nm). The resolved feature, tip convoluted, displays a 1.2 nm height.

demonstrated a clear orientational effect of the cysteine mutation and partial delipidation combination.[29]

Applied forces in the range of 6 − 40 nN ± 2 nN were tested when engaging partially delipidated BR_{cys} with a metal-coated AFM probe, and reliable electrical contact was established at 10−15 nN of contact force. The current flowing through partially delipidated molecular BR_{cys} studied here reached +10 and −10 nA at +1 and −1 V bias, respectively (Figure 2a). After sample engagement in the dark, the light source [495 nm long pass filter, absorption maximum of BR_{cys} (Supporting Information, Figure S1)] was switched on, inducing a conductance increase which decays when the light is switched off. Junction resistances, quantified from a linear fit at the ±0.2 V bias section of $I-V$ curves (Figure 2b), drop by approximately 3-fold from 137 ± 28 MΩ pre-excitation to 39 ± 12 MΩ on illumination. The statistical distribution of the "dark" and "light" resistances showed that light-induced fluctuation was reproducible over some 42 BR_{cys} junctions (Figure 3). Indeed, multiple successive measurements over illumination cycles of ~5 s interspersed with measurements in the dark, on a same

dx.doi.org/10.1021/nl203965w | Nano Lett. XXXX, XXX, XXX−XXX

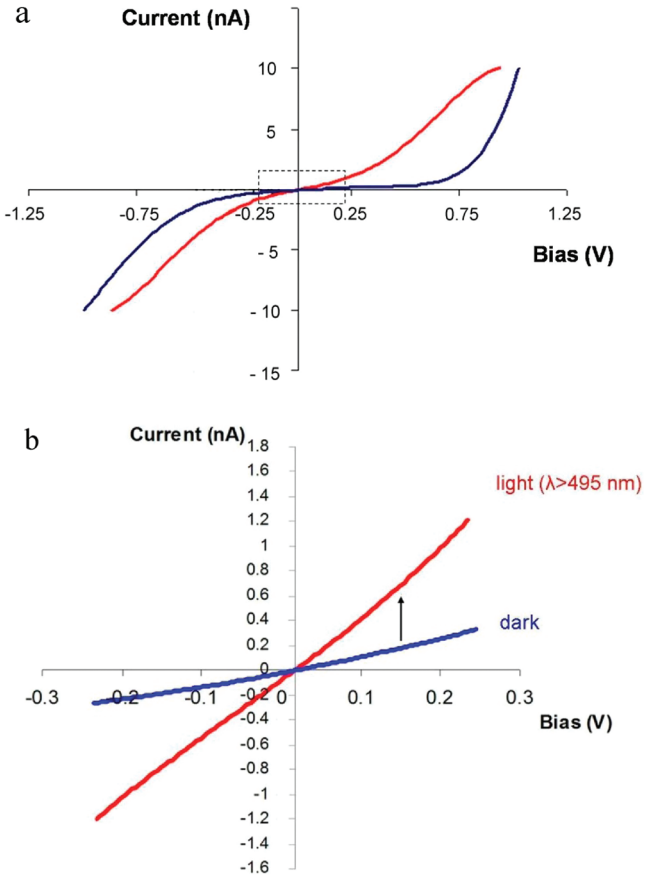

Figure 2. *I*−*V* spectroscopy of partially delipidated BR_{cys} in dark and under illumination using a 495 nm long pass filter. (a) Averaged *I*−*V* curves obtained in the dark (blue) and on illumination (red) during successive illumination cycles of 5 s each. Data shown here from an average of 240 "light" and 260 "dark" curves at a junction force of 15 nN ± 1.3 nN over 42 gold−BR_{cys}−gold junctions; bias range ±1 V, sweep rate =0.5s. (b) Magnification of the linear part of the *I*−*V* curves (±0.2 V bias section, represented by the "boxed" region in a); an increase of conductance is clearly visible on illumination (black arrow). Data analysis showed that the resistance of the molecular junction switched from 137 ± 28 MΩ in the dark, to 39 ± 12 MΩ under illumination. The current switching was not detected at other wavelengths nor for retinal-free BR_{cys} (Supporting Information, Figures S4 and S5), showing the crucial role in conductance of the chromophore, and that the phenomenon is color sensitive.

BR_{cys} junction without withdrawing the tip, lead to a reproducible series of shifts in conductance observable for typically 5 full cycles (Figure 4) and confirming retention of molecular photoactivity through the process. In most cases, a gradual decrease in conductance was observed for junctions following 5−10 dark-light switching cycles, an observation independent of illumination time. Conductance and its photomodulation, however, were robustly reinstated on moving the probe to a different part of the BR modified surface. This observation suggests that the progressive conductance decrease was due to a local current saturation of the protein under the C-AFM probe, rather than being illumination-induced, since the whole sample was illuminated.

The photoinduced conductance switching in these junctions is demonstrably wavelength and retinal-activity tethered: engaging the same BR_{cys} molecules while illuminating through a 550 nm long pass filter resulted in *I*−*V* curves showing no significant shift of conductance (Supporting Information, Figure S4). Similarly, retinal-free partially delipidated BR_{cys} samples, photobleached in the presence of hydroxylamine, showed not only much lower inherent conductance (∼60 pA at +1 V) but also an absence of its modulation on illumination (Supporting Information, Figure S5a,b).

The ability of (redox active) metal sites in proteins to both facilitate facile tunneling conductance across the structure and its electrochemical gating is known.[18] Electronic current across an uncompressed BR molecule spans some 5 nm and is not expected to be significant whether superexchange or hopping pathways are dominant. Despite this, recent analyses have concluded that the lipidated protein can sustain current magnitudes comparable to those observable with conjugated organics of comparable length.[30] The probe-independent observations we report herein not only highlight the role of the retinal moiety in mediating electronic conductance through BR[20] but also the significance of partial delipidation in facilitating a more robust coupling of this conduit to electrodes. The combined effects of partial delipidation and chemisorption on BR electrical properties, long-term stability and on the different intermediates of its photocycle are currently under study.

The ability of surface confined organic chromophores to present a means of photoswitching conductance has generated a good deal of interest in recent years. We have shown here not only that a biologically and technologically important biomolecule can be largely stripped of lipids and anchored in an

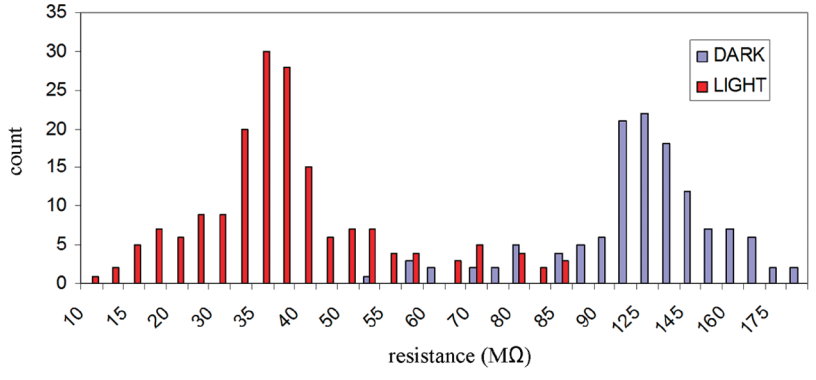

Figure 3. Resistance distribution of 75% delipidated BR_{cys} in dark and light conditions (>495 nm). Only *I*−*V* curves presenting a symmetrical shape toward positive and negative bias were retained for data processing. These curves were analyzed by a computed fit enabling the calculation of individual resistances. This distribution confirms the ∼3-fold drop of resistance, from 137 ± 28 to 39 ± 12 MΩ, observed for trimers of BR_{cys} on illumination (long pass filter cut off at 495 nm, results obtained from 42 BR_{cys} junctions for an applied force of 15 ± 1.3 nN, as in Figure 2).

dx.doi.org/10.1021/nl203965w | *Nano Lett.* XXXX, XXX, XXX−XXX

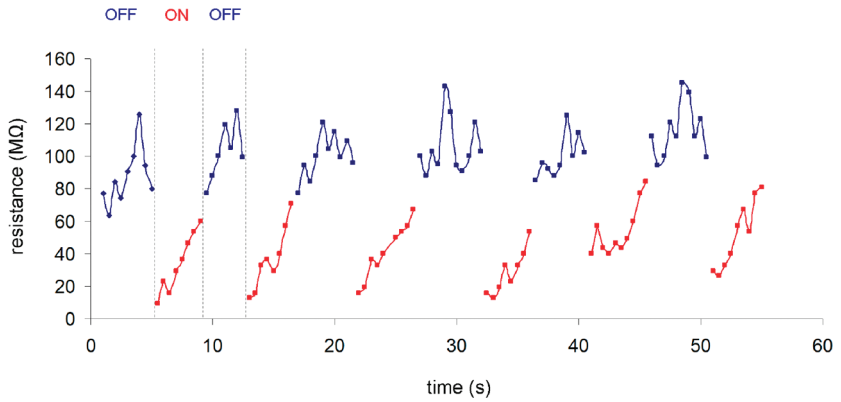

Figure 4. Switching of one BR_{cys} junction resistance under dark and light (>495 nm) conditions over time measured by C-AFM. A drop of resistance is clearly visible on illumination and is reproducibly observed for an average of five cycles of interspersed illuminations. Following cycles showed an attenuation of the shifts probably due to the current saturation (see text). Repeating the experiment on another point of the sample restored the photoswitching behavior. The BR_{cys}-modified gold substrate was engaged at a force of 9 ± 1.2 nN under an applied bias ranging from ±1 V. Each point corresponds to the resistance of single *I*−*V* curves recorded every 0.5s. At 7.5 s (after 15 consecutive *I*−*V* sweeps), a light source fitted with a 495 nm long pass filter was switched on for a few (~4 − 5) seconds and then turned off. C-AFM measurements were performed over successive on/off periods of illumination, which were of slightly variable duration as switching of the light source was performed manually.

orientated and functionally competent form to man made electrodes but also that the molecular conductance of BR can be both measured and reversibly photoswitched with predictable wavelength sensitivity.

Methods. *Sample Preparation.* Wild-type BR and BR_{cys} were grown in peptone media and purified following standard procedures.[3]

Removal of 75% of membrane lipids was achieved by centrifuging the native sample (20900 rpm, 40 min, 4 °C), discarding the supernatant and resolubilizing the pellet in 50% (w/v), 20 mM of 3-[(3-cholamidopropyl)dimethylammonio]-1-propanesulfonate (CHAPS) detergent. The preparation was kept overnight at 4 °C under gentle stirring and the process was repeated twice. The last incubation in detergent was followed by several washes in distilled water, and the protein was then stored at 4 °C.

Removal of the retinal chromophore from the protein (bleached BR_{cys}) was obtained by adding 0.2 M of hydroxylamine (pH of 7.0) to the partially delipidated BR mutant and stirring under a halogen lamp placed at ~10 cm from the sample. Bleaching was performed in a cold room (4 °C) to prevent excessive heating of the sample by the proximity of the halogen lamp. Completion of the reaction was visually detectable by a change in the sample color from deep purple to beige after 30 min. The preparation was then centrifuged and washed several times in distilled water to remove hydroxylamine. After bleaching, the maximum of absorbance shifted from 560 to 360 nm, as expected.[31]

C-AFM. *I*−*V* spectroscopy was performed on a Molecular Imaging Pico STM instrument (Agilent Technologies) using a 1196 AFMS scanner and on a NanoWizard AFM fitted with a C-AFM module (JPK, Germany) at different times. Illumination was performed with a light source (KL 1500 halogen cold light source, 150 W, Schott), whose light guide was fitted onto the microscope at the substrate level for direct illumination of the sample. Experiments were performed in a dark room. Soft contact silicon conducting AFM probes with an overall gold coating and a spring constant of 0.2 N/m (Budget Sensors, Bulgaria) were cleaned for 30 min in a UV cleaning box (Bioforce UV/Ozone ProCleaner, U.S.A.) before use. Gold-on-glass substrates (2 nm rms; Arrandee, Germany) were cleaned in the UV/ozone box for 30 min, washed with ethanol followed by deionized water, and then annealed to obtain atomically flat gold terraces. Annealing was performed by passing a flame over the substrate for a few seconds, gold face up; a process repeated 2−3 times. The substrate was then allowed to cool down to ambient temperature before being incubated overnight at 4 °C in 10 μM of protein solution. The substrates were then thoroughly washed with deionized water, dried under nitrogen, and glued onto a metallic disk. Nitrogen was flown in the microscope chamber of the Agilent system before starting the experiment to reduce the level of humidity. The conducting tip was then brought into contact at low force (1 nN), and surface characterization was performed in contact mode C-AFM. The substrate was partially scanned at constant voltage (scanning intentionally limited to protect the clean probe gold coating) in order to obtain height and current images and thus localize the partially delipidated protein on the surface. Between 5 and 45 BR_{cys} junctions were probed for each substrate. Preliminary *I*−*V* spectroscopy was performed in order to determine the minimum range of forces that should be applied to the sample so reproducible *I*−*V* curves would be generated; this was in the range of 6−10 nN. A force of 15 nN was then systematically applied during the experiments, unless stated otherwise. A voltage bias ranging from −1.5 to +1.5 V was applied to the sample, and the sweep duration was set up at 0.5 s. *I*−*V* curves were first obtained in the dark, and the light was then switched on for ~5 s (GG495 and OG550 long-pass filters, SCHOTT) before being switched off. "On/off" cycles were performed manually, hence a slight difference in each illumination cycle duration. Raw data were analyzed with a home written MatLab routine (R2008b, MathWorks) that selected the predominantly linear *I*−*V* response regime (between −0.2 to 0.2 V for backward and forward sweeps) and computed a linear fit, thus enabling the calculation of the ohmic resistance for each *I*−*V* curve. The results of the *I*−*V* analysis were then collated and further statistically analyzed.

■ ASSOCIATED CONTENT

Supporting Information

UV−vis absorption spectra of partially delipidated BR_{cys} before and after adsorption on transparent gold; gold−BR_{cys}−gold junction characterization; SPR results, ellipsometry, and reductive

dx.doi.org/10.1021/nl203965w | *Nano Lett.* XXXX, XXX, XXX−XXX

stripping methods and results; C-AFM conductance measurements performed on partially delipidated BR_{cys} at a different wavelength and on bleached (retinal-free), partially delipidated BR are provided. This material is available free of charge via the Internet at http://pubs.acs.org.

AUTHOR INFORMATION

Corresponding Author

*E-mail: jason.davis@chem.ox.ac.uk; anthony.watts@bioch.ox.ac.uk

ACKNOWLEDGMENTS

Authors acknowledge support from the EPSRC (studentship fees to O.B.) and the Oxford University EPA Fund for support for W.X. and A.P.

REFERENCES

(1) Palczewski, K.; Kumasaka, T.; Hori, T.; Behnke, C., A.; Motoshima, H.; Fox, B., A.; Le Trong, I.; Teller, D. C.; Okada, T.; Stenkamp, R.; Yamamoto, M.; Miyano, M. Crystal Structure of Rhodopsin: A G Protein-Coupled Receptor. *Science* **2000**, *289*, 739−745.

(2) Essen, L. O.; Mailliet, J.; Hughes, J. The structure of a complete phytochrome sensory module in the Pr ground state. *Proc. Natl. Acad. Sci. U.S.A.* **2008**, *105* (38), 14709−14.

(3) Oesterhelt, D.; Stoeckenius, W. Isolation of the cell membrane of Halobacterium halobium and its fractionation into red and purple membrane. *Methods Enzymol.* **1974**, *31* (Pt A), 667−78.

(4) Henderson, R.; Baldwin, J. M.; Ceska, T. A.; Zemlin, F.; Beckmann, E.; Downing, K. H. Model for the Structure of Bacteriorhodopsin Based on High-Resolution Electron Cryomicroscopy. *J. Mol. Biol.* **1990**, *213* (4), 899−929.

(5) Belrhali, H.; Nollert, P.; Royant, A.; Menzel, C.; Rosenbusch, J. P.; Landau, E. M.; Pebay-Peyroula, E. Protein, lipid and water organization in bacteriorhodopsin crystals: a molecular view of the purple membrana at 1.9 angstrom resolution. *Structure* **1999**, *7* (8), 909−917.

(6) Luecke, H.; Schobert, B.; Richter, H. T.; Cartailler, J. P.; Lanyi, J. K. Structure of bacteriorhodopsin at 1.55 angstrom resolution. *J. Mol. Biol.* **1999**, *291* (4), 899−911.

(7) Hampp, N. Bacteriorhodopsin as a photochromic retinal protein for optical memories. *Chem. Rev.* **2000**, *100* (5), 1755−1776.

(8) Heyes, C. D.; El-Sayed, M. A. The role of the native lipids and lattice structure in bacteriorhodopsin protein conformation and stability as studied by temperature-dependent Fourier transform-infrared spectroscopy. *J. Biol. Chem.* **2002**, *277* (33), 29437−43.

(9) Kates, M. The phytanyl ether-linked polar lipids and isoprenoid neutral lipids of extremely halophilic bacteria. *Prog. Chem. Fats Other Lipids* **1978**, *15* (4), 301−42.

(10) Brown, L. S.; Needleman, R.; Lanyi, J. K. Conformational change of the E-F interhelical loop in the M photointermediate of bacteriorhodopsin. *J. Mol. Biol.* **2002**, *317* (3), 471−8.

(11) Shibata, M.; Uchihashi, T.; Yamashita, H.; Kandori, H.; Ando, T. Structural changes in bacteriorhodopsin in response to alternate illumination observed by high-speed atomic force microscopy. *Angew. Chem., Int. Ed. Engl.* **2011**, *50* (19), 4410−3.

(12) Voitchovsky, K.; Antoranz Contera, S.; Kamihira, M.; Watts, A.; Ryan, J. F. Differential stiffness and lipid mobility in the leaflets of purple membranes. *Biophys. J.* **2006**, *90* (6), 2075−85.

(13) Thorgeirsson, T. E.; Xiao, W.; Brown, L. S.; Needleman, R.; Lanyi, J. K.; Shin, Y. K. Transient channel-opening in bacteriorhodopsin: an EPR study. *J. Mol. Biol.* **1997**, *273* (5), 951−7.

(14) Braun-Sand, S.; Sharma, P. K.; Chu, Z. T.; Pisliakov, A. V.; Warshel, A. The energetics of the primary proton transfer in bacteriorhodopsin revisited: It is a sequential light-induced charge separation after all. *Biochim. Biophys. Acta, Bioenerg.* **2008**, *1777* (5), 441−452.

(15) Tsuchiya, S. Intramolecular Electron Transfer of Diporphyrins Comprised of Electron-Deficient Porphyrin and Electron-Rich Porphyrin with Photocontrolled Isomerization. *J. Am. Chem. Soc.* **1999**, *121* (1), 48−53.

(16) Reddy, D., R.; Maiya, G. A molecular photoswitch based on an'axial-bonding' type phosphorus(V) porphyrin. *Chem. Commun.* **2000**, *1*, 117−118.

(17) Lee, I.; Lee, J. W.; Stubna, A.; Greenbaum, E. Measurement of electrostatic potentials above oriented single photosynthetic reaction centers. *J. Phys. Chem. B* **2000**, *104* (11), 2439−2443.

(18) Davis, J. J.; Morgan, D. A.; Wrathmell, C. L.; Axford, D. N.; Zhao, J.; Wang, N. Molecular Biolelectronics. *J. Mater. Chem.* **2005**, *15* (22), 2160−2174.

(19) Davis, J. J.; Hill, H. A. The scanning probe microscopy of metalloproteins and metalloenzymes. *Chem. Commun. (Camb)* **2002**, *5*, 393−401.

(20) Jin, Y. D.; Friedman, N.; Sheves, M.; He, T.; Cahen, D. Bacteriorhodopsin (bR) as an electronic conduction medium: Current transport through bR-containing monolayers. *Proc. Natl. Acad. Sci. U.S.A.* **2006**, *103* (23), 8601−8606.

(21) Zhao, J. W.; Davis, J. J. Force dependent metalloprotein conductance by conducting atomic force microscopy. *Nanotechnology* **2003**, *14* (9), 1023−1028.

(22) Zhao, J.; Davis, J. J.; Sansom, M. S.; Hung, A. Exploring the electronic and mechanical properties of protein using conducting atomic force microscopy. *J. Am. Chem. Soc.* **2004**, *126* (17), 5601−9.

(23) Casuso, I.; Fumagalli, L.; Samitier, J.; Padrós, E.; Reggiani, L.; Akimov, V.; Gomila, G. Electron transport through supported biomembranes at the nanoscale by conductive atomic force microscopy *Nanotechnology* **2007**, *18*, (46), 465503−10.

(24) Jin, Y.; Honig, T.; Ron, I.; Friedman, N.; Sheves, M.; Cahen, D. Bacteriorhodopsin as an electronic conduction medium for biomolecular electronics. *Chem. Soc. Rev.* **2008**, *37* (11), 2422−32.

(25) Nagy, K. Photoelectric activity of dried, oriented layers of purple membrane from Halobacterium halobium. *Biochem. Biophys. Res. Commun.* **1978**, *85* (1), 383−90.

(26) Varo, G.; Keszthelyi, L. Photoelectric Signals from Dried Oriented Purple Membranes of Halobacterium-Halobium. *Biophys. J.* **1983**, *43* (1), 47−51.

(27) Chen, Z. P.; Birge, R. R. Protein-Based Artificial Retinas. *Trends Biotechnol.* **1993**, *11* (7), 292−300.

(28) Wang, W.; Knopf, W.; Bassi, G. K.; Toward, A. S. mimicking biological vision with protein-based flexible imaging arrays. *Proc. SPIE* **2007**, 8527.

(29) Patil, A.; Premaruban, T.; Berthoumieu, O.; Watts, A.; Davis, J. J., Enhanced photocurrent in engineered bacteriorhodopsin monolayer; *J Phys Chem B*. DOI: 10.1021/jp210520k.

(30) Ron, I.; Pecht, I.; Sheves, M.; Cahen, D. Proteins as Solid-State Electronic Conductors. *Acc. Chem. Res.* **2010**, *43* (7), 945−953.

(31) Moller, C.; Buldt, G.; Dencher, N. A.; Engel, A.; Muller, D. J. Reversible loss of crystallinity on photobleaching purple membrane in the presence of hydroxylamine. *J. Mol. Biol.* **2000**, *301* (4), 869−879.